ILASS–Europe 2022, 31th Conference on Liquid Atomization and Spray Systems, 6-8 September 2022, Virtual, Israel

Water Drop Shaped Like a Crystal Ball

Merav Arogeti*[1], Alexander Shapiro[1]
[1]Mechanical Engineering Department, Shamoon College of Engineering, Beer Sheva, Israel
*Corresponding author: meravar@sce.ac.il

Abstract
A water drop on a small cylindrical pillar reminds of a crystal ball on a stand and creates a hydrophobic effect. Different drop volume generates various contact angles with a pillar made of a non-hydrophobic substance. The contact angles change from a large angle, which is considered hydrophobic, to a minimal hydrophilic angle until the end of the drop evaporating. The pillar's top edge and the drop create the edge effect proposed by Gibbs; the drop's triple contact line is pinned to the sharp edges.
We followed the first stage of the evaporation, the volume loss, which is the main stage using drops on different pillar diameters and a big flat surface. The contact angle changed according to the drop volume. The comparison revealed non-dimensional relation between the volume and the contact angle.

Keywords
Pillar, Evaporation, Contact angle, Edge Effect

Introduction

Pillars, as small targets, have a unique influence on water drop behavior due to the flip in the ratio of the dimensions; the drop diameter is equal to or bigger than the target diameter. The natural evaporation allows us to observe gradual changes in the drop volume on different pillars. We are specifically interested in the TCL (Triple Contact Line) and the CA (Contact Angle) changes.
The literature divided the drop evaporation on the surface into stages. At the initial stage, the TCL is pinned, and the CA decreases. The following stage depends on the surface and ambient properties; therefore, different studies reported similar but not identical descriptions. The TCL is de-pinned and decreases with the CA, for metal surface At a CA of about 20°[1]. Other studies found that the receding CA is the minimal CA that remains constant, and only the TCL decreases [2]. A third stage is defined for small volume, and all parameters decrease [3], [4].
Gibbs, in 1906, defined the contact angle hysteresis for drop encountering a sharp edge by geometrical inequality condition [5].

$$\theta_0 \leq \theta \leq (180° - \phi) + \theta_0 \qquad (1)$$

Where the equilibrium contact angle is θ_0 and ϕ is the angle between the surfaces that generate the solid edge, which is $90°$ for the pillars in this study.
The sharp edge effect for drops on pillars is studied in different aspects, such as how geometry can enhance the TCL pinning effect [6], the geometrical effect of the pillar section cut [7], and the coffee ring effect by the drop evaporation [8]. We studied the similarities and differences between the drop edge effect and evaporation on two small pillars and a big surface.

Material and Methods

Triple distilled water drop positioned on high polished top of tool steel cylindrical pillar. Before every experiment, the pillar working surface was polished on sandpaper with 1200/2000 grit up to a mirror state. The pillar was cleaned by rinsing in tap water, drying, rinsing in ethanol, and drying.

The examined pillar's diameters are 1.2 mm, 2.4mm as small targets, and 6mm, a larger diameter than the examined drop's maximal spread and considered a big surface. Each drop evaporated under similar ambient conditions, and we recorded the process.

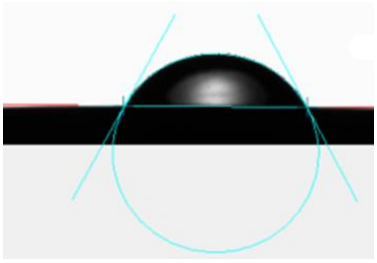

Figure 1. Measured equivalent CA of drop on big surface

We measured the initial CA of a drop laying on a big surface, which is the equivalent CA, $\theta_0 = 61.5°$. The drop did not reach the edges, and the equivalent CA applies to all experiments with the same solid surface and liquid drop (see **Figure 1**). We defined non-dimensional volume to normalize the pillar differences, the ratio between the measured drop volume at any time $V(t)$ and the volume measured at the equivalent CA during the evaporation, defined as the reference volume, $V(\theta_0)$.

Results and Discussion

The shape of the water drop on a surface is round and truncated. Drop on pillars can generate various contact angles even over 90 degrees, angles that are considered hydrophobic (see **Figure 2**, left side).

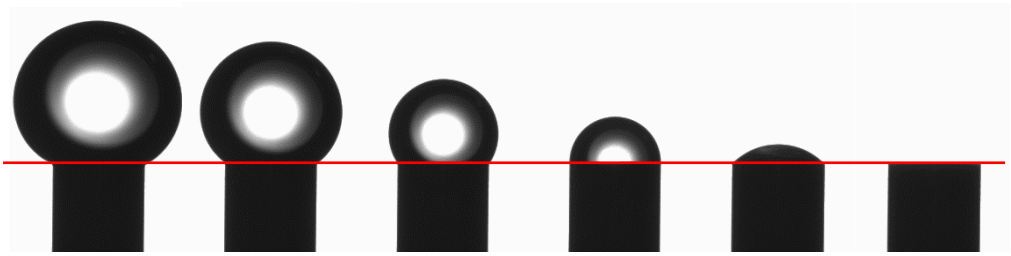

Figure 2. Liquid drop evaporation on a pillar

The pillar's sharp edge enables this large contact angle, even though the pillar substance is not hydrophobic. The contact angle values were described by Gibbs inequality (see **Equation 1**) and used for sharp edges analysis [8]–[10]. The achieved stable drop for large CA agrees with Gibbs inequality high limits $(90° + \theta_0)$. We placed a drop with an initial CA of $110°$ on the pillar (2.4mm) and added water in doses of 0.01µL. Initially, the CA increased with the volume up to the maximal CA and maintained with additional volume. At a certain point, the drop lost its symmetrical position with a minor contact angle reduction, which was the stability loss trigger, and the drop on the pillar collapsed (see **Figure 3**).

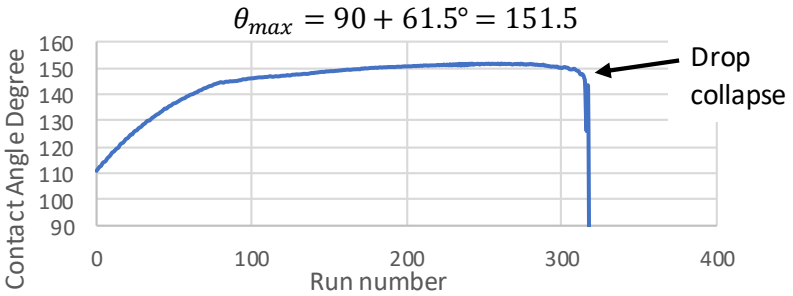

Figure 3. Drop contact angle during increasing the drop volume until stability limit

All our trails to generate stable CA a larger than Gibbs θ_{max} , failed; also, a close value was Hard to achieve stability due to the sensitivity of the drop at those values. Therefore, our evaporation experiments begin with a smaller angle.

The Gibbs inequality low angle is the equivalent CA and represents the lower initial CA for a fresh drop. Aged drop during the evaporation process can generate smaller CA.

The values and relations between the horizontal surface area and the drop volume determine the drop roundness. We compared drops on two pillars with a CA of a 125°. Symmetric positioning of the drop keeps the whole drop on the surface top, and the TCL is along the pillar's upper edge. The ratio between the diameters of the examined pillars is similar to all the geometrical properties ratios between the drops, the drop volumes, maximal diameters, and maximal heights (see **Figure 4**).

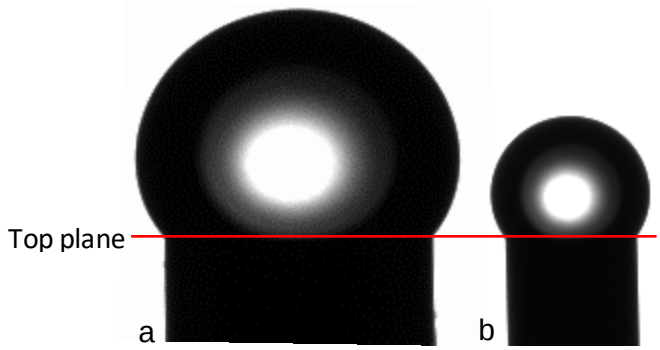

Figure 4. All drops' Contact angle are 125° a) 2.4mm pillar diameter b) 1.2mm pillar diameter

We followed the changes in the CA during evaporation. The first stage of drop evaporation from pillar is similar to the big plane surface pinned TCL and decreases in contact angle (see **Figure 2**).

The following stages, which end with complete evaporation, should be studied separately; different recording paces and image magnifying are required. In agreement with the literature, our observation indicates that the next stage begins with CA approximately at 20°. The following stages last a short period, while the TCL and CA of the drop decrease until the liquid evaporates.

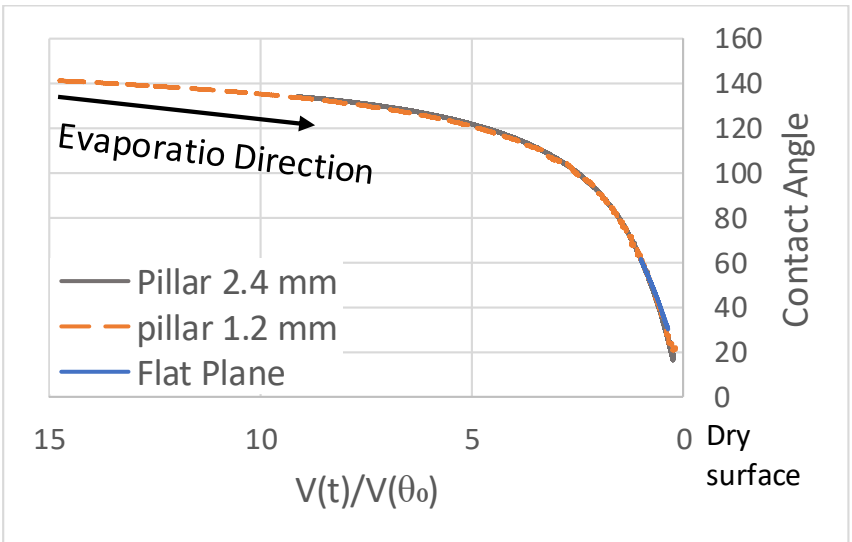

Figure 5. Contact angle during evaporation vs. none-dimensional volume for different surfaces, all curves unify.

Focus on the first stage shows that the CA changes along the non-dimensional volume evaporation unify for all examined surfaces, two pillars, and a big surface (see **Figure 5**). Each experiment began with a different CA depending on the ability to achieve a stable drop. For the big surface, the maximal initial CA is the equivalent CA. The curves unify with no regard to the drop age; each contact angle relates to the same non-dimensional volume. To enhance the conclusion about the drop age, we compared similar drops distinct only by the initial volume on the same pillar and found that all drops have the same relations between similar values of CA and volume.

The pillar edge creates a hydrophobic effect. The drop lays on the pillar, like a crystal ball, and therefore accumulates more liquid volume per contact area than a surface without sharp edge. At the hydrophobic CA, the drop losses most of its volume with a light changes in the contact angle. In the range of 100° to 80 °, as the drop CA changes to hydrophilic, the tendency gradually changes and flips rate, and the contact angle decreases faster.

Occasionally the drop TCL may exceed the pillar's horizontal surface [5]. The TCL descends along the pillar circumference (see **Figure 6**). We found that the deviation from the pillar top occurs when the drop is placed asymmetrically. Therefore, the TCL is a three-dimensional curved line pinned during the evaporation to the pillar's vertical wall. Even though the contact is along the vertical wall, traditionally, the CA measured refers to the horizontal plane from the contact height [5] and not to the vertical wall (see **Figure 6c)**. The deviation from the horizontal plane is slight, and most drop volume lies on the horizontal plane. This method enables consistent analysis of the drop characteristics and evaporation process. The TCL on the vertical wall creates a partial coating of the pillar, which enlarge the free surface area for

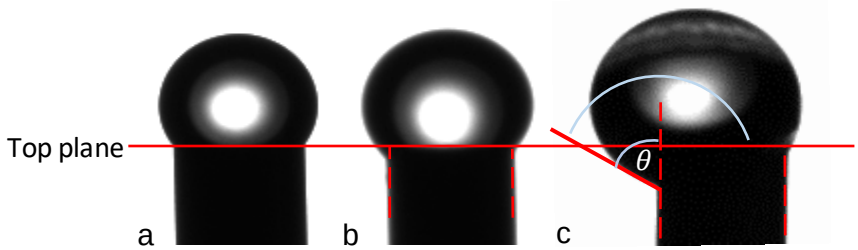

Figure 6. All drops' on 1.2 mm pillar, the drop position changes the TCL location a) symmetric b) slightly asymmetric c) extremely asymmetric

evaporation. The contact angles along the TCL varies with significant differences between the pillar sides. Therefore, the maximal angle we measured was close to the maximal angle defined by Gibbs inequality for a sharp corner. Achieving a stable maximal angle was easier for asymmetrical drop positioning.

Conclusions

We confirmed the CA stability limit by Gibbs inequality for a drop on a sharp edge. The drop's geometrical proportions are the same between different pillars: CA, height, diameter, and the relative drop volume. The CA reduction during volume lost by the first stage of drop evaporation unifies all non-dimensional volume with no regard to the plane dimensions or the drop age.

Acknowledgments

This work was supported by the Authority for Research and Development at Shamoon College of Engineering.

Nomenclature

θ	Contact angle (CA)
θ_0	Equilibrium CA
ϕ	Angle between the edge surfaces
$V(t)$	Drop volume at any time
$V(\theta_0)$	Drop volume at Equilibrium CA

References

[1] E. Bormashenko, A. Musin, and M. Zinigrad, 2011, *Colloids and Surfaces A: Physicochemical and Engineering Aspects*, 385(1–3), pp. 235–240.
[2] S. Chandra, " M di Marzo, Y. M. Qiao, and & P. Tartarini, 1996, Fire safety journal, 27(2) pp.141-158 .
[3] J. K. Park, J. Ryu, B. C. Koo, S. Lee, and K. H. Kang, 2012, *Soft Matter*, 8(47), pp. 11889–11896.
[4] C. Bourgks-Monnier and M. E. R. Shanahan, 1995, *Langmuir*, 11(7), pp. 2820–2829.
[5] J. F. Oliver, C. Huh, and S. G. Mason, 1977, *Journal of Colloid and Interface Science*, 59(3), pp. 568–581.
[6] Z. Wang, K. Lin, and Y. P. Zhao, 2019, *Journal of Colloid and Interface Science*, 552, pp. 563–571.
[7] T. Tóth *et al.*, 2011, *Langmuir*, 27(8), pp. 4742–4748
[8] I. Sandu, C. T. Fleacă, F. Dumitrache, B. Sava, I. Urzică, and M. Dumitru, 2021, *Applied Physics A: Materials Science and Processing*, 127(5), pp. 1–9.
[9] J. Granã-Otero and I. E. Parra Fabián, 2019, *Physical Review Fluids*, 4(11).
[10] G. Fang and A. Amirfazli, 2012, *Langmuir*, 28(25), pp. 9421–9430.